

PDF hosted at the Radboud Repository of the Radboud University Nijmegen

The following full text is a publisher's version.

For additional information about this publication click this link.

<http://hdl.handle.net/2066/128944>

Please be advised that this information was generated on 2017-12-05 and may be subject to change.

Measurement of CP -Violating Asymmetries in B^0 Decays to CP Eigenstates

B. Aubert,¹ D. Boutigny,¹ I. De Bonis,¹ J.-M. Gaillard,¹ A. Jeremie,¹ Y. Karyotakis,¹ J. P. Lees,¹ P. Robbe,¹ V. Tisserand,¹ A. Palano,² G. P. Chen,³ J. C. Chen,³ N. D. Qi,³ G. Rong,³ P. Wang,³ Y. S. Zhu,³ G. Eigen,⁴ P. L. Reinertsen,⁴ B. Stugu,⁴ B. Abbott,⁵ G. S. Abrams,⁵ A. W. Borgland,⁵ A. B. Breon,⁵ D. N. Brown,⁵ J. Button-Shafer,⁵ R. N. Cahn,⁵ A. R. Clark,⁵ S. Dardin,⁵ C. Day,⁵ S. F. Dow,⁵ T. Elioff,⁵ Q. Fan,⁵ I. Gaponenko,⁵ M. S. Gill,⁵ F. R. Goosen,⁵ S. J. Gowdy,⁵ A. Gritsan,⁵ Y. Groysman,⁵ R. G. Jacobsen,⁵ R. C. Jared,⁵ R. W. Kadel,⁵ J. Kadyk,⁵ A. Karcher,⁵ L. T. Kerth,⁵ I. Kipnis,⁵ S. Kluth,⁵ Yu. G. Kolomensky,⁵ J. F. Kral,⁵ R. Lafever,⁵ C. LeClerc,⁵ M. E. Levi,⁵ S. A. Lewis,⁵ C. Lionberger,⁵ T. Liu,⁵ M. Long,⁵ G. Lynch,⁵ M. Marino,⁵ K. Marks,⁵ A. B. Meyer,⁵ A. Mokhtarani,⁵ M. Momayezi,⁵ M. Nyman,⁵ P. J. Oddone,⁵ J. Ohnemus,⁵ D. Oshatz,⁵ S. Patton,⁵ A. Perazzo,⁵ C. Peters,⁵ W. Pope,⁵ M. Pripstein,⁵ D. R. Quarrie,⁵ J. E. Rasson,⁵ N. A. Roe,⁵ A. Romosan,⁵ M. T. Ronan,⁵ V. G. Shelkov,⁵ R. Stone,⁵ A. V. Telnov,⁵ H. von der Lippe,⁵ T. Weber,⁵ W. A. Wenzel,⁵ M. S. Zisman,⁵ P. G. Bright-Thomas,⁶ T. J. Harrison,⁶ C. M. Hawkes,⁶ A. Kirk,⁶ D. J. Knowles,⁶ S. W. O'Neale,⁶ A. T. Watson,⁶ N. K. Watson,⁶ T. Deppermann,⁷ H. Koch,⁷ J. Krug,⁷ M. Kunze,⁷ B. Lewandowski,⁷ K. Peters,⁷ H. Schmucker,⁷ M. Steinke,⁷ J. C. Andress,⁸ N. R. Barlow,⁸ W. Bhimji,⁸ N. Chevalier,⁸ P. J. Clark,⁸ W. N. Cottingham,⁸ N. De Groot,⁸ N. Dyce,⁸ B. Foster,⁸ A. Mass,⁸ J. D. McFall,⁸ D. Wallom,⁸ F. F. Wilson,⁸ K. Abe,⁹ C. Hearty,⁹ T. S. Mattison,⁹ J. A. McKenna,⁹ D. Thiessen,⁹ B. Camanzi,¹⁰ S. Jolly,¹⁰ A. K. McKemey,¹⁰ J. Tinslay,¹⁰ V. E. Blinov,¹¹ A. D. Bukin,¹¹ D. A. Bukin,¹¹ A. R. Buzykaev,¹¹ M. S. Dubrovin,¹¹ V. B. Golubev,¹¹ V. N. Ivanchenko,¹¹ G. M. Kolachev,¹¹ A. A. Korol,¹¹ E. A. Kravchenko,¹¹ A. P. Onuchin,¹¹ A. A. Salnikov,¹¹ S. I. Serednyakov,¹¹ Yu. I. Skovpen,¹¹ V. I. Telnov,¹¹ A. N. Yushkov,¹¹ A. J. Lankford,¹² M. Mandelkern,¹² S. McMahon,¹² D. P. Stoker,¹² A. Ahsan,¹³ C. Buchanan,¹³ S. Chun,¹³ D. B. MacFarlane,¹⁴ S. Prell,¹⁴ Sh. Rahatlou,¹⁴ G. Raven,¹⁴ V. Sharma,¹⁴ S. Burke,¹⁵ C. Campagnari,¹⁵ B. Dahmes,¹⁵ D. Hale,¹⁵ P. A. Hart,¹⁵ N. Kuznetsova,¹⁵ S. Kyre,¹⁵ S. L. Levy,¹⁵ O. Long,¹⁵ A. Lu,¹⁵ J. D. Richman,¹⁵ W. Verkerke,¹⁵ M. Witherell,¹⁵ S. Yellin,¹⁵ J. Beringer,¹⁶ D. E. Dorfan,¹⁶ A. M. Eisner,¹⁶ A. Frey,¹⁶ A. A. Grillo,¹⁶ M. Grothe,¹⁶ C. A. Heusch,¹⁶ R. P. Johnson,¹⁶ W. Kroeger,¹⁶ W. S. Lockman,¹⁶ T. Pulliam,¹⁶ H. Sadrozinski,¹⁶ T. Schalk,¹⁶ R. E. Schmitz,¹⁶ B. A. Schumm,¹⁶ A. Seiden,¹⁶ E. N. Spencer,¹⁶ M. Turri,¹⁶ W. Walkowiak,¹⁶ D. C. Williams,¹⁶ E. Chen,¹⁷ G. P. Dubois-Felsmann,¹⁷ A. Dvoretzskii,¹⁷ J. E. Hanson,¹⁷ D. G. Hitlin,¹⁷ S. Metzler,¹⁷ J. Oyang,¹⁷ F. C. Porter,¹⁷ A. Ryd,¹⁷ A. Samuel,¹⁷ M. Weaver,¹⁷ S. Yang,¹⁷ R. Y. Zhu,¹⁷ S. Devmal,¹⁸ T. L. Geld,¹⁸ S. Jayatilke,¹⁸ S. M. Jayatilke,¹⁸ G. Mancinelli,¹⁸ B. T. Meadows,¹⁸ M. D. Sokoloff,¹⁸ P. Bloom,¹⁹ S. Fahey,¹⁹ W. T. Ford,¹⁹ F. Gaede,¹⁹ W. C. van Hoek,¹⁹ D. R. Johnson,¹⁹ A. K. Michael,¹⁹ U. Nauenberg,¹⁹ A. Olivas,¹⁹ H. Park,¹⁹ P. Rankin,¹⁹ J. Roy,¹⁹ S. Sen,¹⁹ J. G. Smith,¹⁹ D. L. Wagner,¹⁹ J. Blouw,²⁰ J. L. Harton,²⁰ M. Krishnamurthy,²⁰ A. Soffer,²⁰ W. H. Toki,²⁰ D. W. Warner,²⁰ R. J. Wilson,²⁰ J. Zhang,²⁰ T. Brandt,²¹ J. Brose,²¹ T. Colberg,²¹ G. Dahlinger,²¹ M. Dickopp,²¹ R. S. Dubitzky,²¹ P. Eckstein,²¹ H. Fatterschneider,²¹ R. Krause,²¹ E. Maly,²¹ R. Müller-Pfefferkorn,²¹ S. Otto,²¹ K. R. Schubert,²¹ R. Schwierz,²¹ B. Spaan,²¹ L. Wilden,²¹ L. Behr,²² D. Bernard,²² G. R. Bonneaud,²² F. Brochard,²² J. Cohen-Tanugi,²² S. Ferrag,²² G. Fouque,²² F. Gastaldi,²² P. Matricon,²² P. Mora de Freitas,²² C. Renard,²² E. Roussot,²² S. T'Jampens,²² C. Thiebaux,²² G. Vasileiadis,²² M. Verderi,²² A. Anjomshoa,²³ R. Bernet,²³ F. Di Lodovico,²³ A. Khan,²³ F. Muheim,²³ S. Playfer,²³ J. E. Swain,²³ M. Falbo,²⁴ C. Bozzi,²⁵ S. Dittongo,²⁵ M. Folegani,²⁵ L. Piemontese,²⁵ E. Treadwell,²⁶ F. Anulli,^{27,*} R. Baldini-Ferrolì,²⁷ A. Calcaterra,²⁷ R. de Sangro,²⁷ D. Falciai,²⁷ G. Finocchiaro,²⁷ P. Patteri,²⁷ I. M. Peruzzi,^{27,*} M. Piccolo,²⁷ Y. Xie,²⁷ A. Zallo,²⁷ S. Bagnasco,²⁸ A. Buzzo,²⁸ R. Contri,²⁸ G. Crosetti,²⁸ M. Lo Vetere,²⁸ M. Macri,²⁸ M. R. Monge,²⁸ M. Pallavicini,²⁸ S. Passaggio,²⁸ F. C. Pastore,²⁸ C. Patrignani,²⁸ M. G. Pia,²⁸ E. Robutti,²⁸ A. Santroni,²⁸ M. Morii,²⁹ R. Bartoldus,³⁰ T. Dignan,³⁰ R. Hamilton,³⁰ U. Mallik,³⁰ J. Cochran,³¹ H. B. Crawley,³¹ P. A. Fischer,³¹ J. Lamsa,³¹ R. McKay,³¹ W. T. Meyer,³¹ E. I. Rosenberg,³¹ J. N. Albert,³² C. Beigbeder,³² M. Benkebil,³² D. Breton,³² R. Cizeron,³² S. Du,³² G. Grosdidier,³² C. Hast,³² A. Höcker,³² V. LePeltier,³² A. M. Lutz,³² S. Plaszczynski,³² M. H. Schune,³² S. Trincas-Duvoid,³² K. Truong,³² A. Valassi,³² G. Wormser,³² R. M. Bionta,³³ V. Brigljević,³³ A. Brooks,³³ O. Fackler,³³ D. Fujino,³³ D. J. Lange,³³ M. Mugge,³³ T. G. O'Connor,³³ B. Pedrotti,³³ X. Shi,³³ K. van Bibber,³³ T. J. Wenaus,³³ D. M. Wright,³³ C. R. Wuest,³³ B. Yamamoto,³³ M. Carroll,³⁴ J. R. Fry,³⁴ E. Gabathuler,³⁴ R. Gamet,³⁴ M. George,³⁴ M. Kay,³⁴ D. J. Payne,³⁴ R. J. Sloane,³⁴ C. Touramanis,³⁴ M. L. Aspinwall,³⁵ D. A. Bowerman,³⁵ P. D. Dauncey,³⁵ U. Egede,³⁵ I. Eschrich,³⁵ N. J. W. Gunawardane,³⁵ R. Martin,³⁵ J. A. Nash,³⁵ D. R. Price,³⁵ P. Sanders,³⁵ D. Smith,³⁵ D. E. Azzopardi,³⁶ J. J. Back,³⁶ P. Dixon,³⁶ P. F. Harrison,³⁶ D. Newman-Coburn,³⁶ R. J. L. Potter,³⁶ H. W. Shorthouse,³⁶ P. Strother,³⁶ P. B. Vidal,³⁶ M. I. Williams,³⁶ G. Cowan,³⁷ S. George,³⁷ M. G. Green,³⁷ A. Kurup,³⁷ C. E. Marker,³⁷ P. McGrath,³⁷ T. R. McMahon,³⁷ F. Salvatore,³⁷ I. Scott,³⁷

G. Vaitsas,³⁷ D. Brown,³⁸ C. L. Davis,³⁸ K. Ford,³⁸ Y. Li,³⁸ J. Pavlovich,³⁸ J. Allison,³⁹ R. J. Barlow,³⁹ J. T. Boyd,³⁹ J. Fullwood,³⁹ F. Jackson,³⁹ G. D. Lafferty,³⁹ N. Savvas,³⁹ E. T. Simopoulos,³⁹ R. J. Thompson,³⁹ J. H. Weatherall,³⁹ R. Bard,⁴⁰ A. Farbin,⁴⁰ A. Jawahery,⁴⁰ V. Lillard,⁴⁰ J. Olsen,⁴⁰ D. A. Roberts,⁴⁰ J. R. Schieck,⁴⁰ G. Blaylock,⁴¹ C. Dallapiccola,⁴¹ K. T. Flood,⁴¹ S. S. Hertzbach,⁴¹ R. Kofler,⁴¹ C. S. Lin,⁴¹ H. Staengle,⁴¹ S. Willocq,⁴¹ J. Wittlin,⁴¹ B. Brau,⁴² R. Cowan,⁴² G. Sciolla,⁴² F. Taylor,⁴² R. K. Yamamoto,⁴² D. I. Britton,⁴³ M. Milek,⁴³ P. M. Patel,⁴³ J. Trischuk,⁴³ F. Lanni,⁴⁴ F. Palombo,⁴⁴ J. M. Bauer,⁴⁵ M. Booke,⁴⁵ L. Cremaldi,⁴⁵ V. Eschenberg,⁴⁵ R. Kroeger,⁴⁵ M. Reep,⁴⁵ J. Reidy,⁴⁵ D. A. Sanders,⁴⁵ D. J. Summers,⁴⁵ M. Beaulieu,⁴⁶ J. P. Martin,⁴⁶ J. Y. Nief,⁴⁶ R. Seitz,⁴⁶ P. Taras,⁴⁶ V. Zacek,⁴⁶ H. Nicholson,⁴⁷ C. S. Sutton,⁴⁷ N. Cavallo,^{48,†} C. Cartaro,⁴⁸ G. De Nardo,⁴⁸ F. Fabozzi,⁴⁸ C. Gatto,⁴⁸ L. Lista,⁴⁸ P. Paolucci,⁴⁸ D. Piccolo,⁴⁸ C. Sciacca,⁴⁸ J. M. LoSecco,⁴⁹ J. R. G. Alsmiller,⁵⁰ T. A. Gabriel,⁵⁰ T. Handler,⁵⁰ J. Heck,⁵⁰ J. E. Brau,⁵¹ R. Frey,⁵¹ M. Iwasaki,⁵¹ N. B. Sinev,⁵¹ D. Strom,⁵¹ E. Borsato,⁵² F. Colecchia,⁵² F. Dal Corso,⁵² F. Galeazzi,⁵² M. Margoni,⁵² M. Marzolla,⁵² G. Michelon,⁵² M. Morandin,⁵² M. Posocco,⁵² M. Rotondo,⁵² F. Simonetto,⁵² R. Stroili,⁵² E. Torassa,⁵² C. Voci,⁵² P. Bailly,⁵³ M. Benayoun,⁵³ H. Briand,⁵³ J. Chauveau,⁵³ P. David,⁵³ C. De la Vaissière,⁵³ L. Del Buono,⁵³ J. F. Genat,⁵³ O. Hamon,⁵³ F. Le Diberder,⁵³ H. Lebbolo,⁵³ Ph. Leruste,⁵³ J. Lory,⁵³ L. Martin,⁵³ L. Roos,⁵³ J. Stark,⁵³ S. Versillé,⁵³ B. Zhang,⁵³ P. F. Manfredi,⁵⁴ L. Ratti,⁵⁴ V. Re,⁵⁴ V. Speziali,⁵⁴ E. D. Frank,⁵⁵ L. Gladney,⁵⁵ Q. H. Guo,⁵⁵ J. H. Panetta,⁵⁵ C. Angelini,⁵⁶ G. Batignani,⁵⁶ S. Bettarini,⁵⁶ M. Bondioli,⁵⁶ F. Bosi,⁵⁶ M. Carpinelli,⁵⁶ F. Forti,⁵⁶ M. A. Giorgi,⁵⁶ A. Lusiani,⁵⁶ F. Martinez-Vidal,⁵⁶ M. Morganti,⁵⁶ N. Neri,⁵⁶ E. Paoloni,⁵⁶ M. Rama,⁵⁶ G. Rizzo,⁵⁶ F. Sandrelli,⁵⁶ G. Simi,⁵⁶ G. Triggiani,⁵⁶ J. Walsh,⁵⁶ M. Haire,⁵⁷ D. Judd,⁵⁷ K. Paick,⁵⁷ L. Turnbull,⁵⁷ D. E. Wagoner,⁵⁷ J. Albert,⁵⁸ C. Bula,⁵⁸ R. Fernholz,⁵⁸ C. Lu,⁵⁸ K. T. McDonald,⁵⁸ V. Miftakov,⁵⁸ B. Sands,⁵⁸ S. F. Schaffner,⁵⁸ A. J. S. Smith,⁵⁸ A. Tumanov,⁵⁸ E. W. Varnes,⁵⁸ F. Bronzini,⁵⁹ A. Buccheri,⁵⁹ C. Bulfon,⁵⁹ G. Cavoto,⁵⁹ D. del Re,⁵⁹ R. Faccini,^{14,59} F. Ferrarotto,⁵⁹ F. Ferroni,⁵⁹ K. Fratini,⁵⁹ E. Lamanna,⁵⁹ E. Leonardi,⁵⁹ M. A. Mazzoni,⁵⁹ S. Morganti,⁵⁹ G. Piredda,⁵⁹ F. Safai Tehrani,⁵⁹ M. Serra,⁵⁹ C. Voena,⁵⁹ R. Waldi,⁶⁰ P. F. Jacques,⁶¹ M. Kalelkar,⁶¹ R. J. Plano,⁶¹ T. Adye,⁶² B. Claxton,⁶² B. Franek,⁶² S. Galagedera,⁶² N. I. Geddes,⁶² G. P. Gopal,⁶² J. Lidbury,⁶² S. M. Xella,⁶² R. Aleksan,⁶³ P. Besson,^{63,‡} P. Bourgeois,⁶³ G. De Domenico,⁶³ S. Emery,⁶³ A. Gaidot,⁶³ S. F. Ganzhur,⁶³ L. Gosset,⁶³ G. Hamel de Monchenault,⁶³ W. Kozanecki,⁶³ M. Langer,⁶³ G. W. London,⁶³ B. Mayer,⁶³ B. Serfass,⁶³ G. Vasseur,⁶³ C. Yeche,⁶³ M. Zito,⁶³ N. Coptly,⁶⁴ M. V. Purohit,⁶⁴ H. Singh,⁶⁴ F. X. Yumiceva,⁶⁴ I. Adam,⁶⁵ P. L. Anthony,⁶⁵ D. Aston,⁶⁵ K. Baird,⁶⁵ J. Bartelt,⁶⁵ J. Becla,⁶⁵ R. Bell,⁶⁵ E. Bloom,⁶⁵ C. T. Boeheim,⁶⁵ A. M. Boyarski,⁶⁵ R. F. Boyce,⁶⁵ F. Bulos,⁶⁵ W. Burgess,⁶⁵ B. Byers,⁶⁵ G. Calderini,⁶⁵ R. Claus,⁶⁵ M. R. Convery,⁶⁵ R. Coombes,⁶⁵ L. Cottrell,⁶⁵ D. P. Coupal,⁶⁵ D. H. Coward,⁶⁵ W. W. Craddock,⁶⁵ H. DeStaebler,⁶⁵ J. Dorfan,⁶⁵ M. Doser,⁶⁵ W. Dunwoodie,⁶⁵ S. Ecklund,⁶⁵ T. H. Fieguth,⁶⁵ R. C. Field,⁶⁵ D. R. Freytag,⁶⁵ T. Glanzman,⁶⁵ G. L. Godfrey,⁶⁵ P. Grosso,⁶⁵ G. Haller,⁶⁵ A. Hanushevsky,⁶⁵ J. Harris,⁶⁵ A. Hasan,⁶⁵ J. L. Hewett,⁶⁵ T. Himel,⁶⁵ M. E. Huffer,⁶⁵ W. R. Innes,⁶⁵ C. P. Jessop,⁶⁵ H. Kawahara,⁶⁵ L. Keller,⁶⁵ M. H. Kelsey,⁶⁵ P. Kim,⁶⁵ L. A. Klaisner,⁶⁵ M. L. Kocian,⁶⁵ H. J. Krebs,⁶⁵ P. F. Kunz,⁶⁵ U. Langenegger,⁶⁵ W. Langeveld,⁶⁵ D. W. G. S. Leith,⁶⁵ S. K. Louie,⁶⁵ S. Luitz,⁶⁵ V. Luth,⁶⁵ H. L. Lynch,⁶⁵ J. MacDonald,⁶⁵ G. Manzin,⁶⁵ H. Marsiske,⁶⁵ M. McCulloch,⁶⁵ D. McShurley,⁶⁵ S. Menke,⁶⁵ R. Messner,⁶⁵ S. Metcalfe,⁶⁵ K. C. Moffeit,⁶⁵ R. Mount,⁶⁵ D. R. Muller,⁶⁵ D. Nelson,⁶⁵ M. Nordby,⁶⁵ C. P. O'Grady,⁶⁵ F. G. O'Neill,⁶⁵ G. Oxoby,⁶⁵ T. Pavel,⁶⁵ J. Perl,⁶⁵ S. Petrak,⁶⁵ G. Putallaz,⁶⁵ H. Quinn,⁶⁵ P. E. Raines,⁶⁵ B. N. Ratcliff,⁶⁵ R. Reif,⁶⁵ S. H. Robertson,⁶⁵ L. S. Rochester,⁶⁵ A. Roodman,⁶⁵ J. J. Russell,⁶⁵ L. Sapozhnikov,⁶⁵ O. H. Saxton,⁶⁵ T. Schietinger,⁶⁵ R. H. Schindler,⁶⁵ J. Schwiening,⁶⁵ J. T. Seeman,⁶⁵ V. V. Serbo,⁶⁵ K. Skarpass, Sr.,⁶⁵ A. Snyder,⁶⁵ A. Soha,⁶⁵ S. M. Spanier,⁶⁵ A. Stahl,⁶⁵ J. Stelzer,⁶⁵ D. Su,⁶⁵ M. K. Sullivan,⁶⁵ M. Talby,⁶⁵ H. A. Tanaka,⁶⁵ J. Va'vra,⁶⁵ S. R. Wagner,⁶⁵ A. J. R. Weinstein,⁶⁵ J. L. White,⁶⁵ U. Wienands,⁶⁵ W. J. Wisniewski,⁶⁵ C. C. Young,⁶⁵ G. Zioulas,⁶⁵ P. R. Burchat,⁶⁶ C. H. Cheng,⁶⁶ D. Kirkby,⁶⁶ T. I. Meyer,⁶⁶ C. Roat,⁶⁶ A. De Silva,⁶⁷ R. Henderson,⁶⁷ S. Berridge,⁶⁸ W. Bugg,⁶⁸ H. Cohn,⁶⁸ E. Hart,⁶⁸ A. W. Weidemann,⁶⁸ T. Benninger,⁶⁹ J. M. Izen,⁶⁹ I. Kitayama,⁶⁹ X. C. Lou,⁶⁹ M. Turcotte,⁶⁹ F. Bianchi,⁷⁰ M. Bona,⁷⁰ B. Di Girolamo,⁷⁰ D. Gamba,⁷⁰ A. Smol,⁷⁰ D. Zanin,⁷⁰ L. Bosisio,⁷¹ G. Della Ricca,⁷¹ L. Lanceri,⁷¹ A. Pompili,⁷¹ P. Poropat,⁷¹ G. Vuagnin,⁷¹ R. S. Panvini,⁷² C. M. Brown,⁷³ R. Kowalewski,⁷³ J. M. Roney,⁷³ H. R. Band,⁷⁴ E. Charles,⁷⁴ S. Dasu,⁷⁴ P. Elmer,⁷⁴ H. Hu,⁷⁴ J. R. Johnson,⁷⁴ J. Nielsen,⁷⁴ W. Orejudos,⁷⁴ Y. Pan,⁷⁴ R. Prepost,⁷⁴ I. J. Scott,⁷⁴ J. H. von Wimmersperg-Toeller,⁷⁴ S. L. Wu,⁷⁴ Z. Yu,⁷⁴ H. Zobernig,⁷⁴ T. M. B. Kordich,⁷⁵ T. B. Moore,⁷⁵ and H. Neal⁷⁵

(BABAR Collaboration)

¹Laboratoire de Physique des Particules, F-74941 Annecy-le-Vieux, France

²Università di Bari, Dipartimento di Fisica and INFN, I-70126 Bari, Italy

³Institute of High Energy Physics, Beijing 100039, China

⁴Institute of Physics, University of Bergen, N-5007 Bergen, Norway

⁵Lawrence Berkeley National Laboratory and University of California, Berkeley, California 94720

- ⁶University of Birmingham, Birmingham B15 2TT, United Kingdom
- ⁷Ruhr Universität Bochum, Institut für Experimentalphysik I, D-44780 Bochum, Germany
- ⁸University of Bristol, Bristol BS8 1TL, United Kingdom
- ⁹University of British Columbia, Vancouver, British Columbia, Canada V6T 1Z1
- ¹⁰Brunel University, Uxbridge, Middlesex UB8 3PH, United Kingdom
- ¹¹Budker Institute of Nuclear Physics, Novosibirsk 630090, Russia
- ¹²University of California at Irvine, Irvine, California 92697
- ¹³University of California at Los Angeles, Los Angeles, California 90024
- ¹⁴University of California at San Diego, La Jolla, California 92093
- ¹⁵University of California at Santa Barbara, Santa Barbara, California 93106
- ¹⁶Institute for Particle Physics, University of California at Santa Cruz, Santa Cruz, California 95064
- ¹⁷California Institute of Technology, Pasadena, California 91125
- ¹⁸University of Cincinnati, Cincinnati, Ohio 45221
- ¹⁹University of Colorado, Boulder, Colorado 80309
- ²⁰Colorado State University, Fort Collins, Colorado 80523
- ²¹Technische Universität Dresden, Institut für Kern- u. Teilchenphysik, D-01062 Dresden, Germany
- ²²Ecole Polytechnique, F-91128 Palaiseau, France
- ²³University of Edinburgh, Edinburgh EH9 3JZ, United Kingdom
- ²⁴Elon College, Elon College, North Carolina 27244-2010
- ²⁵Dipartimento di Fisica and INFN, Università di Ferrara, I-44100 Ferrara, Italy
- ²⁶Florida A&M University, Tallahassee, Florida 32307
- ²⁷Laboratori Nazionali di Frascati dell'INFN, I-00044 Frascati, Italy
- ²⁸Dipartimento di Fisica and INFN, Università di Genova, I-16146 Genova, Italy
- ²⁹Harvard University, Cambridge, Massachusetts 02138
- ³⁰University of Iowa, Iowa City, Iowa 52242-3160
- ³¹Iowa State University, Ames, Iowa 50011
- ³²Laboratoire de l'Accélérateur Linéaire, F-91898 Orsay, France
- ³³Lawrence Livermore National Laboratory, Livermore, California 94550
- ³⁴University of Liverpool, Liverpool L69 3BX, United Kingdom
- ³⁵University of London, Imperial College, London SW7 2BW, United Kingdom
- ³⁶Queen Mary, University of London, London E1 4NS, United Kingdom
- ³⁷University of London, Royal Holloway, and Bedford New College, Egham, Surrey TW20 0EX, United Kingdom
- ³⁸University of Louisville, Louisville, Kentucky 40292
- ³⁹University of Manchester, Manchester M13 9PL, United Kingdom
- ⁴⁰University of Maryland, College Park, Maryland 20742
- ⁴¹University of Massachusetts, Amherst, Massachusetts 01003
- ⁴²Lab for Nuclear Science, Massachusetts Institute of Technology, Cambridge, Massachusetts 02139
- ⁴³McGill University, Montréal, Canada QC H3A 2T8
- ⁴⁴Dipartimento di Fisica and INFN, Università di Milano, I-20133 Milano, Italy
- ⁴⁵University of Mississippi, University, Mississippi 38677
- ⁴⁶Laboratoire René J.A. Lévesque, Université de Montréal, Montréal, Canada QC H3C 3J7
- ⁴⁷Mount Holyoke College, South Hadley, Massachusetts 01075
- ⁴⁸Dipartimento di Scienze Fisiche and INFN, Università di Napoli Federico II, I-80126 Napoli, Italy
- ⁴⁹University of Notre Dame, Notre Dame, Indiana 46556
- ⁵⁰Oak Ridge National Laboratory, Oak Ridge, Tennessee 37831
- ⁵¹University of Oregon, Eugene, Oregon 97403
- ⁵²Dipartimento di Fisica and INFN, Università di Padova, I-35131 Padova, Italy
- ⁵³Lab de Physique Nucléaire H.E., Universités Paris VI et VII, F-75252 Paris, France
- ⁵⁴Dipartimento di Elettronica and INFN, Università di Pavia, I-27100 Pavia, Italy
- ⁵⁵University of Pennsylvania, Philadelphia, Pennsylvania 19104
- ⁵⁶Scuola Normale Superiore and INFN, Università di Pisa, I-56010 Pisa, Italy
- ⁵⁷Prairie View A&M University, Prairie View, Texas 77446
- ⁵⁸Princeton University, Princeton, New Jersey 08544
- ⁵⁹Dipartimento di Fisica and INFN, Università di Roma La Sapienza, I-00185 Roma, Italy
- ⁶⁰Universität Rostock, D-18051 Rostock, Germany
- ⁶¹Rutgers University, New Brunswick, New Jersey 08903
- ⁶²Rutherford Appleton Laboratory, Chilton, Didcot, Oxon OX11 0QX, United Kingdom
- ⁶³DAPNIA, Commissariat à l'Energie Atomique/Saclay, F-91191 Gif-sur-Yvette, France
- ⁶⁴University of South Carolina, Columbia, South Carolina 29208
- ⁶⁵Stanford Linear Accelerator Center, Stanford, California 94309
- ⁶⁶Stanford University, Stanford, California 94305-4060
- ⁶⁷TRIUMF, Vancouver, British Columbia, Canada V6T 2A3

⁶⁸University of Tennessee, Knoxville, Tennessee 37996⁶⁹University of Texas at Dallas, Richardson, Texas 75083⁷⁰Dipartimento di Fisica Sperimentale and INFN, Università di Torino, I-10125 Torino, Italy⁷¹Dipartimento di Fisica and INFN, Università di Trieste, I-34127 Trieste, Italy⁷²Vanderbilt University, Nashville, Tennessee 37235⁷³University of Victoria, Victoria, British Columbia, Canada V8W 3P6⁷⁴University of Wisconsin, Madison, Wisconsin 53706⁷⁵Yale University, New Haven, Connecticut 06511

(Received 12 February 2001)

We present measurements of time-dependent CP -violating asymmetries in neutral B decays to several CP eigenstates. The measurement uses a data sample of 23×10^6 $Y(4S) \rightarrow B\bar{B}$ decays collected by the $BABAR$ detector at the PEP-II asymmetric B Factory at SLAC. In this sample, we find events in which one neutral B meson is fully reconstructed in a CP eigenstate containing charmonium and the flavor of the other neutral B meson is determined from its decay products. The amplitude of the CP -violating asymmetry, which in the standard model is proportional to $\sin 2\beta$, is derived from the decay time distributions in such events. The result is $\sin 2\beta = 0.34 \pm 0.20$ (stat) ± 0.05 (syst).

DOI: 10.1103/PhysRevLett.86.2515

PACS numbers: 13.25.Hw, 12.15.Hh, 11.30.Er

CP -violating asymmetries in the time distributions of decays of B^0 and \bar{B}^0 mesons provide a direct test of the standard model of electroweak interactions [1]. For the neutral B decay modes reported here, corrections to CP -violating effects from strong interactions are absent, in contrast to the K_L^0 modes in which CP violation was discovered [2].

Using a data sample of 23×10^6 $B\bar{B}$ pairs recorded at the $Y(4S)$ resonance by the $BABAR$ detector at the PEP-II asymmetric-energy e^+e^- collider at the Stanford Linear Accelerator Center, we have fully reconstructed a sample B_{CP} of neutral B mesons decaying to the CP eigenstates $J/\psi K_s^0$, $\psi(2S)K_s^0$, and $J/\psi K_L^0$. We examine each of the events in this sample for evidence that the other neutral B meson decayed as a B^0 or a \bar{B}^0 , designated as a B^0 or \bar{B}^0 flavor tag. The final B_{CP} sample contains about 360 signal events.

When the $Y(4S)$ decays, the P -wave $B\bar{B}$ state evolves coherently until one of the mesons decays. In one of

four time-order and flavor configurations, if the tagging meson B_{tag} decays first, and as a B^0 , the other meson must be a \bar{B}^0 at that same time t_{tag} . It then evolves independently and can decay into a CP eigenstate B_{CP} at a later time t_{CP} . The time between the two decays $\Delta t = t_{CP} - t_{\text{tag}}$ is a signed quantity made measurable by producing the $Y(4S)$ with a boost $\beta\gamma = 0.56$ along the collision (z) axis, with nominal energies of 9.0 and 3.1 GeV for the electron and positron beams. The measured distance $\Delta z \approx \beta\gamma c \Delta t$ between the two decay vertices provides a good estimate of the corresponding time interval Δt ; the average value of $|\Delta z|$ is $\beta\gamma c \tau_{B^0} \approx 250 \mu\text{m}$.

The decay-time distribution for events with a B^0 or a \bar{B}^0 tag can be expressed in terms of a complex parameter λ that depends on both $B^0\bar{B}^0$ mixing and on the amplitudes describing \bar{B}^0 and B^0 decay to a common final state f [3]. The distribution $f_+(f_-)$ of the decay rate when the tagging meson is a $B^0(\bar{B}^0)$ is given by

$$f_{\pm}(\Delta t) = \frac{e^{-|\Delta t|/\tau_{B^0}}}{2\tau_{B^0}(1 + |\lambda|^2)} \times \left[\frac{1 + |\lambda|^2}{2} \pm \text{Im}\lambda \sin(\Delta m_{B^0}\Delta t) \mp \frac{1 - |\lambda|^2}{2} \cos(\Delta m_{B^0}\Delta t) \right], \quad (1)$$

where τ_{B^0} is the B^0 lifetime and Δm_{B^0} is the mass difference determined from $B^0\bar{B}^0$ mixing [4], and where the lifetime difference between neutral B mass eigenstates is assumed to be negligible. The first oscillatory term in Eq. (1) is due to interference between direct decay and decay after mixing. A difference between the B^0 and \bar{B}^0 distributions or a Δt asymmetry for either tag is evidence for CP violation.

If all amplitudes contributing to $B^0 \rightarrow f$ have the same weak phase, a condition satisfied in the standard model for charmonium-containing $b \rightarrow c\bar{c}s$ decays, then $|\lambda| = 1$. For these CP eigenstates the standard model predicts $\lambda = \eta_f e^{-2i\beta}$, where η_f is the CP eigenvalue of the state f and $\beta = \arg[-V_{cd}V_{cb}^*/V_{td}V_{tb}^*]$ is an angle of the unitarity triangle of the three-generation Cabibbo-Kobayashi-Maskawa (CKM) matrix [5]. Thus, the time-dependent CP -violating asymmetry is

$$A_{CP}(\Delta t) \equiv \frac{f_+(\Delta t) - f_-(\Delta t)}{f_+(\Delta t) + f_-(\Delta t)} = -\eta_f \sin 2\beta \sin(\Delta m_{B^0}\Delta t), \quad (2)$$

where $\eta_f = -1$ for $J/\psi K_s^0$ and $\psi(2S)K_s^0$ and $+1$ for $J/\psi K_L^0$.

A measurement of A_{CP} requires determination of the experimental Δt resolution and the fraction of events in which the tag assignment is incorrect. A mistag fraction w reduces the observed asymmetry by a factor $(1 - 2w)$.

Several samples of fully reconstructed B^0 mesons are used in this measurement. The B_{CP} sample contains candidates reconstructed in the CP eigenstates $J/\psi K_s^0(K_s^0 \rightarrow \pi^+\pi^-, \pi^0\pi^0)$, $\psi(2S)K_s^0(K_s^0 \rightarrow \pi^+\pi^-)$, and $J/\psi K_L^0$. The J/ψ and $\psi(2S)$ mesons are reconstructed through their decays to e^+e^- and $\mu^+\mu^-$; the $\psi(2S)$ is

also reconstructed through its decay to $J/\psi \pi^+ \pi^-$. A sample of B decays B_{flav} [6] used in the determination of the mistag fractions and Δt resolution functions consists of the channels $D^{(*)-} h^+ (h^+ = \pi^+, \rho^+, a_1^+)$ and $J/\psi K^{*0} (K^{*0} \rightarrow K^+ \pi^-)$. A control sample of charged B mesons decaying to the final states $J/\psi K^{(*)+}$, $\psi(2S) K^+$, and $\bar{D}^{(*)0} \pi^+$ is used for validation studies.

A description of the *BABAR* detector can be found in Ref. [7]. Charged particles are detected and their momenta measured by a combination of a silicon vertex tracker (SVT) consisting of five double-sided layers and a central drift chamber (DCH), in a 1.5-T solenoidal field. The average vertex resolution in the z direction is 70 μm for a fully reconstructed B meson. We identify leptons and hadrons with measurements from all detector systems, including the energy loss (dE/dx) in the DCH and SVT. Electrons and photons are identified by a CsI electromagnetic calorimeter (EMC). Muons are identified in the instrumented flux return (IFR). A Cherenkov ring imaging detector (DIRC) covering the central region, together with the dE/dx information, provides K - π separation of at least 3 standard deviations for B decay products with momentum greater than 250 MeV/c in the laboratory.

We select events with a minimum of three reconstructed charged tracks, each having a laboratory polar angle between 0.41 and 2.54 rad and an impact parameter in the plane transverse to the beam less than 1.5 cm from the beam line. The event must have a total measured energy in the laboratory greater than 4.5 GeV within the fiducial regions for charged tracks and neutral clusters. To help reject continuum background, the second Fox-Wolfram moment [8] must be less than 0.5.

An electron candidate must have a ratio of calorimeter energy to track momentum, an EMC cluster shape, a DCH dE/dx , and a DIRC Cherenkov angle (if available) consistent with an electron.

A muon candidate must satisfy requirements on the measured and expected number of interaction lengths penetrated, the position match between the extrapolated DCH track and IFR hits, and the average and spread of the number of IFR hits per layer.

A track is identified as a kaon candidate by means of a neural network that uses dE/dx measurements in the DCH and SVT, and comparison of the observed pattern of detected photons in the DIRC with that expected for kaon and pion hypotheses.

Candidates for $J/\psi \rightarrow \ell^+ \ell^-$ must have at least one decay product identified as a lepton (electron or muon) candidate or, if outside the calorimeter acceptance, must have DCH dE/dx information consistent with the electron hypothesis. Tracks in which the electron has radiated are combined with bremsstrahlung photons, reconstructed as clusters with more than 30 MeV lying within 35 mrad in polar angle and 50 mrad in azimuth of the projected photon position on the EMC. The second track of a $\mu^+ \mu^-$ pair, if within the acceptance of the calorimeter, must be consistent with being a minimum ionizing particle. Two iden-

tified electron or muon candidates are required for J/ψ or $\psi(2S) \rightarrow \ell^+ \ell^-$ reconstruction in the higher-background $\psi(2S) K_s^0$ and $J/\psi K_L^0$ channels.

We require a J/ψ candidate to have $2.95 \leq m_{e^+ e^-} \leq 3.14 \text{ GeV}/c^2$ or $3.06 \leq m_{\mu^+ \mu^-} \leq 3.14 \text{ GeV}/c^2$, and a $\psi(2S) \rightarrow \ell^+ \ell^-$ candidate to have $3.44 \leq m_{e^+ e^-} \leq 3.74 \text{ GeV}/c^2$ or $3.64 \leq m_{\mu^+ \mu^-} \leq 3.74 \text{ GeV}/c^2$. Requirements are made on the lepton helicity angle in order to provide further discrimination against background. For the $\psi(2S) \rightarrow J/\psi \pi^+ \pi^-$ mode, mass-constrained J/ψ candidates are combined with pairs of oppositely charged tracks considered as pions; the resulting mass must be within 15 MeV/c^2 of the $\psi(2S)$ mass [4].

A $K_s^0 \rightarrow \pi^+ \pi^-$ candidate must satisfy $489 < m_{\pi^+ \pi^-} < 507 \text{ MeV}/c^2$. The distance between the J/ψ or $\psi(2S)$ and K_s^0 vertices is required to be at least 1 mm.

Pairs of π^0 candidates with total energy above 800 MeV are considered as K_s^0 candidates for the $J/\psi K_s^0$ mode. We determine the most probable K_s^0 decay point along the path defined by the initial K_s^0 momentum vector and the J/ψ vertex by maximizing the product of probabilities for the daughter π^0 mass-constrained fits. Allowing for vertex resolution, we require the displacement from the J/ψ vertex to the decay point to be between -10 and +40 cm and the $\pi^0 \pi^0$ mass evaluated at this point to be between 470 and 550 MeV/c^2 .

A K_L^0 candidate is formed from a cluster not matched to a reconstructed track. For the EMC the cluster must have energy above 200 MeV, while for the IFR the cluster must have at least two layers. We determine the K_L^0 energy by combining its direction with the reconstructed J/ψ momentum, assuming the decay $B^0 \rightarrow J/\psi K_L^0$. To reduce photon backgrounds, EMC clusters consistent with a $\pi^0 \rightarrow \gamma \gamma$ decay are rejected and the transverse missing momentum of the event projected on the K_L^0 candidate direction must be consistent with the K_L^0 momentum. In addition, the center-of-mass J/ψ momentum is required to be greater than 1.4 GeV/c .

B_{CP} candidates used in the analysis are selected by requiring that the difference ΔE between the energy of the B_{CP} candidate and the beam energy in the center-of-mass frame be less than 3 standard deviations from zero and that, for K_s^0 modes, the beam-energy substituted mass $m_{\text{ES}} = \sqrt{(E_{\text{beam}}^{\text{cm}})^2 - (p_B^{\text{cm}})^2}$ must be greater than 5.2 GeV/c^2 . The resolution for ΔE is about 10 MeV, except for $J/\psi K_L^0$ (3 MeV) and the $K_s^0 \rightarrow \pi^0 \pi^0$ mode (33 MeV). For the purpose of determining numbers of events, purities, and efficiencies, a signal region $m_{\text{ES}} > 5.27 \text{ GeV}/c^2$ is used for all modes except $J/\psi K_L^0$.

Figure 1 shows the resulting ΔE and m_{ES} distributions for B_{CP} candidates containing a K_s^0 , and ΔE for the candidates containing a K_L^0 . The B_{CP} sample is composed of 890 events in the signal region, with an estimated background of 260 events, predominantly in the $J/\psi K_L^0$ channel. For that channel, the composition, effective η_f , and ΔE distributions of the individual background sources are

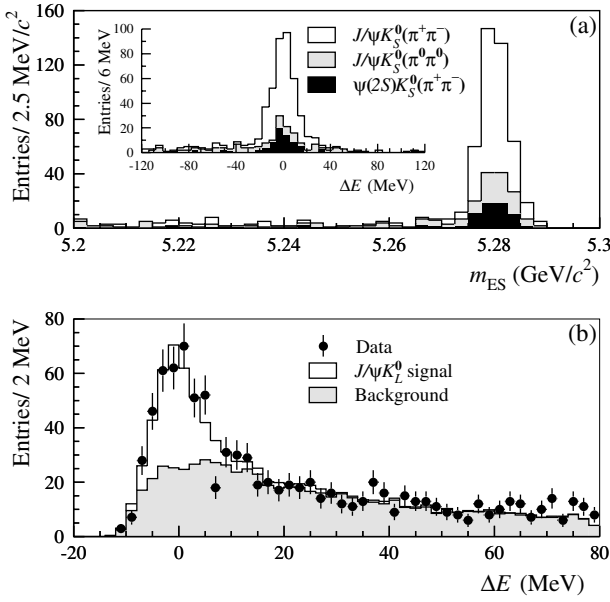


FIG. 1. (a) Distribution of m_{ES} and ΔE for B_{CP} candidates having a K_S^0 in the final state; (b) distribution of ΔE for $J/\psi K_L^0$ candidates.

taken either from a Monte Carlo simulation (for B decays to J/ψ) or from the $m_{\ell^+\ell^-}$ sidebands in data.

For flavor tagging, we exploit information from the incompletely reconstructed other B decay in the event. The charge of energetic electrons and muons from semileptonic B decays, kaons, soft pions from D^* decays, and high momentum charged particles is correlated with the flavor of the decaying b quark: e.g., a positive lepton yields a B^0 tag. Each event is assigned to one of four hierarchical, mutually exclusive tagging categories or is excluded from further analysis. The mistag fractions and efficiencies of all categories are determined from data.

A lepton tag requires an electron or muon candidate with a center-of-mass momentum $p_{cm} > 1.0$ or 1.1 GeV/ c , respectively. This efficiently selects primary leptons and reduces contamination due to oppositely charged leptons from semileptonic charm decays. Events meeting these criteria are assigned to the lepton category unless the lepton charge and the net charge of all kaon candidates indicate opposite tags. Events without a lepton tag but with a nonzero net kaon charge are assigned to the kaon category.

All remaining events are passed to a neural network algorithm whose main inputs are the momentum and charge of the track with the highest center-of-mass momentum, and the outputs of secondary networks, trained with Monte Carlo samples to identify primary leptons, kaons, and soft pions. Based on the output of the neural network algorithm, events are tagged as B^0 or \bar{B}^0 and assigned to the NT1 (more certain tags) or NT2 (less certain tags) category, or not tagged at all. The tagging power of the NT1 and NT2 categories arises primarily from soft pions and from recovering unidentified isolated primary electrons and muons.

Table I shows the number of tagged events and the signal purity, determined from fits to the m_{ES} (K_S^0 modes) or ΔE (K_L^0 mode) distributions. The measured efficiencies for the four tagging categories are summarized in Table II.

The uncertainty in the Δt measurement is dominated by the measurement of the position z_{tag} of the tagging vertex. The tagging vertex is determined by fitting the tracks not belonging to the B_{CP} (or B_{flav}) candidate to a common vertex. Reconstructed K_S^0 and Λ candidates are used as input to the fit in place of their daughters. Tracks from γ conversions are excluded from the fit. To reduce contributions from charm decay, which bias the vertex estimation, the track with the largest vertex χ^2 contribution greater than 6 is removed and the fit is redone until no track fails the χ^2 requirement or fewer than two tracks remain. The average resolution for $\Delta z = z_{CP} - z_{tag}$ is $190 \mu\text{m}$. The time interval Δt between the two B decays is then determined from the Δz measurement, including an event-by-event correction for the direction of the B with respect to the z direction in the $Y(4S)$ frame. An accepted candidate must have a converged fit for the B_{CP} and B_{tag} vertices, an error of less than $400 \mu\text{m}$ on Δz , and a measured $|\Delta z| < 3$ mm; 86% of the B_{CP} events satisfy this requirement.

The $\sin 2\beta$ measurement is made with an unbinned maximum likelihood fit to the Δt distribution of the combined B_{CP} and B_{flav} tagged samples. The Δt distribution of the former is given by Eq. (1), with $|\lambda| = 1$. The latter evolves according to the known rate for flavor oscillations in neutral B mesons. The amplitudes for B_{CP} asymmetries and for B_{flav} flavor oscillations are reduced by the same

TABLE I. Number of tagged events, signal purity, and result of fitting for CP asymmetries in the full CP sample and in various subsamples, as well as in the B_{flav} and charged B control samples. Purity is the fitted number of signal events divided by the total number of events in the ΔE and m_{ES} signal region defined in the text. Errors are statistical only.

Sample	N_{tag}	Purity (%)	$\sin 2\beta$
$J/\psi K_S^0, \psi(2S) K_S^0$	273	96 ± 1	0.25 ± 0.22
$J/\psi K_L^0$	256	39 ± 6	0.87 ± 0.51
Full CP sample	529	69 ± 2	0.34 ± 0.20
$J/\psi K_S^0, \psi(2S) K_S^0$ only			
$J/\psi K_S^0 (K_S^0 \rightarrow \pi^+ \pi^-)$	188	98 ± 1	0.25 ± 0.26
$J/\psi K_S^0 (K_S^0 \rightarrow \pi^0 \pi^0)$	41	85 ± 6	-0.05 ± 0.66
$\psi(2S) K_S^0 (K_S^0 \rightarrow \pi^+ \pi^-)$	44	97 ± 3	0.40 ± 0.50
Lepton tags	34	99 ± 2	0.07 ± 0.43
Kaon tags	156	96 ± 2	0.40 ± 0.29
NT1 tags	28	97 ± 3	-0.03 ± 0.67
NT2 tags	55	96 ± 3	0.09 ± 0.76
B^0 tags	141	96 ± 2	0.24 ± 0.31
\bar{B}^0 tags	132	97 ± 2	0.25 ± 0.30
B_{flav} sample	4637	86 ± 1	0.03 ± 0.05
Charged B sample	5165	90 ± 1	0.02 ± 0.05

TABLE II. Average mistag fractions w_i and mistag differences $\Delta w_i = w_i(B^0) - w_i(\bar{B}^0)$ extracted for each tagging category i from the maximum-likelihood fit to the time distribution for the fully reconstructed B^0 sample ($B_{\text{flav}} + B_{CP}$). The figure of merit for tagging is the effective tagging efficiency $Q_i = \varepsilon_i(1 - 2w_i)^2$, where ε_i is the fraction of events with a reconstructed tag vertex that is assigned to the i th category. Uncertainties are statistical only. The statistical error on $\sin 2\beta$ is proportional to $1/\sqrt{Q}$, where $Q = \sum Q_i$.

Category	ε (%)	w (%)	Δw (%)	Q (%)
Lepton	10.9 ± 0.4	11.6 ± 2.0	3.1 ± 3.1	6.4 ± 0.7
Kaon	36.5 ± 0.7	17.1 ± 1.3	-1.9 ± 1.9	15.8 ± 1.3
NT1	7.7 ± 0.4	21.2 ± 2.9	7.8 ± 4.2	2.6 ± 0.5
NT2	13.7 ± 0.5	31.7 ± 2.6	-4.7 ± 3.5	1.8 ± 0.5
All	68.9 ± 1.0			26.7 ± 1.6

factor $(1 - 2w)$ due to mistags. The distributions are both convoluted with a common Δt resolution function and corrected for backgrounds, incorporated with different assumptions about their Δt evolution and convoluted with a separate resolution function. Events are assigned signal and background probabilities based on fits to m_{ES} (all modes except $J/\psi K_L^0$) or ΔE ($J/\psi K_L^0$) distributions.

The Δt resolution function for signal candidates is represented by a sum of three Gaussian distributions with different means and widths. For the core and tail Gaussians, the widths are scaled by the event-by-event measurement error derived from the vertex fits; the combined rms error is 1.1 ps. A separate offset for the core distribution is allowed for each tagging category to account for small shifts caused by inclusion of residual charm decay products in the tag vertex; a common offset is used for the tail component. The third Gaussian (of fixed 8 ps width) accounts for the fewer than 1% of events with incorrectly reconstructed vertices. Identical resolution function parameters are used for all modes, since the B_{tag} vertex precision dominates the Δt resolution.

A total of 35 parameters are varied in the final fit, including the values of $\sin 2\beta$ (1), the average mistag fraction w and the difference Δw between B^0 and \bar{B}^0 mistags for each tagging category (8), parameters for the signal Δt resolution (9), and parameters for background time dependence (6), Δt resolution (3) and mistag fractions (8). The determination of the mistag fractions and signal Δt resolution function is dominated by the high-statistics B_{flav} sample, while background parameters are governed by events with $m_{ES} < 5.27 \text{ GeV}/c^2$ (except $J/\psi K_L^0$). We fix $\tau_{B^0} = 1.548 \text{ ps}$ and $\Delta m_{B^0} = 0.472 \hbar \text{ ps}^{-1}$ [4]. The largest correlation between $\sin 2\beta$ and any linear combination of the other free parameters is 0.076.

The measurement of $\sin 2\beta$ was performed as a blind analysis by hiding the value of $\sin 2\beta$ obtained from the fit, as well as the CP asymmetry in the Δt distribution, until the analysis was complete. This allowed us to study statistical and systematic errors without knowing the numerical value of $\sin 2\beta$.

The measured mistag rates obtained from the likelihood fit for the four tagging categories are summarized in Table II. As a check, the mistag rates were evaluated

with a sample of about 16 000 $D^{*-} \ell^+ \nu_\ell$ events and found to be consistent with the results from the hadronic decay sample.

The combined fit to the CP decay modes and the flavor decay modes yields

$$\sin 2\beta = 0.34 \pm 0.20 \text{ (stat)} \pm 0.05 \text{ (syst)}.$$

The decay asymmetry A_{CP} as a function of Δt and the log likelihood as a function of $\sin 2\beta$ are shown in Fig. 2. If $|\lambda|$ is allowed to float in the fit, the value obtained is consistent with 1 and there is no significant difference in the value of $-\eta_f \text{Im}\lambda/|\lambda|$ (identified with $\sin 2\beta$ in the standard model) and our quoted result. Repeating the fit with all parameters fixed to their determined values except $\sin 2\beta$, we find that a total contribution of ± 0.02 to the error on $\sin 2\beta$ is due to the combined statistical uncertainties in mistag rates, Δt resolution, and background parameters.

The dominant sources of systematic error are the assumed parametrization of the Δt resolution function (0.04), due in part to residual uncertainties in the SVT alignment, and uncertainties in the level, composition, and CP asymmetry of the background in the selected CP events (0.02). The systematic errors from uncertainties in Δm_{B^0} and τ_{B^0} and from the parametrization of the background in the selected B_{flav} sample are found to be negligible. An increase of $0.02 \hbar \text{ ps}^{-1}$ in the assumed value for Δm_{B^0} decreases $\sin 2\beta$ by 0.012.

The large sample of reconstructed events allows a number of consistency checks, including separation of the data by decay mode, tagging category, and B_{tag} flavor. The results of fits to these subsamples are shown in Table I for the high-purity K_S^0 events. Table I also shows results of fits with the samples of non- CP decay modes, where no statistically significant CP asymmetry is found.

Our measurement of $\sin 2\beta$ is consistent with, but improves substantially on the precision of, previous determinations [9]. The central value is consistent with the range implied by measurements and theoretical estimates of the magnitudes of CKM matrix elements [10]; it is also consistent with no CP asymmetry at the 1.7σ level.

We thank our PEP-II colleagues for their extraordinary achievement in reaching design luminosity and high

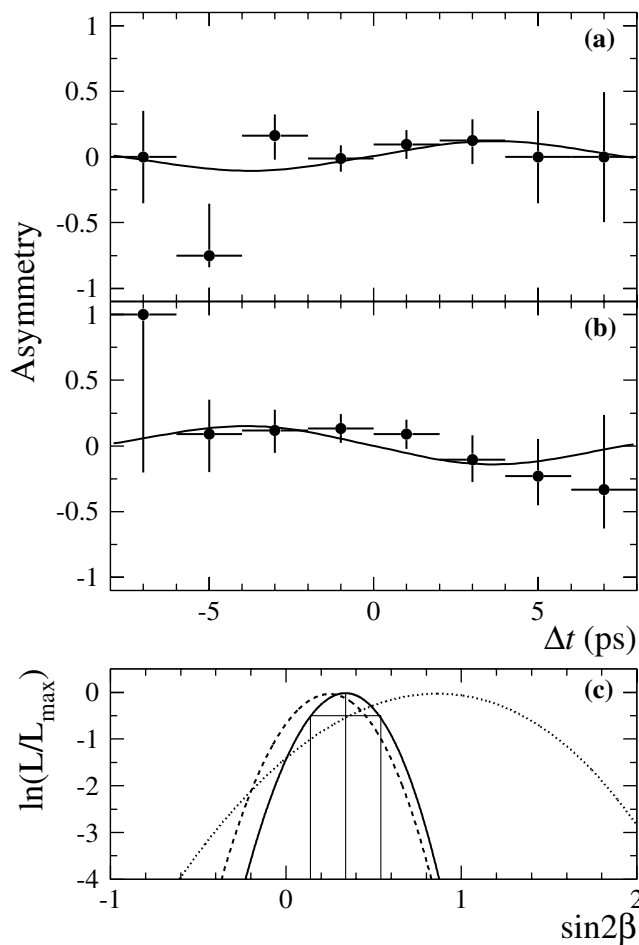


FIG. 2. The raw asymmetry in the number of B^0 and \bar{B}^0 tags in the signal region, $(N_{B^0} - N_{\bar{B}^0})/(N_{B^0} + N_{\bar{B}^0})$, with asymmetric binomial errors, as a function of Δt for (a) the $J/\psi K_S^0$ and $\psi(2S)K_S^0$ modes ($\eta_f = -1$) and (b) the $J/\psi K_L^0$ mode ($\eta_f = +1$). The solid curves represent the time-dependent asymmetries determined for the central values of $\sin 2\beta$ from the fits for these samples. Eight events that lie outside the plotted interval were also used in the fits. The probability of obtaining a lower likelihood, evaluated using a Monte Carlo technique, is 60%. (c) Variation of the log likelihood as a function of $\sin 2\beta$ for the modes containing K_S^0 (dashed curve), the $J/\psi K_L^0$ mode (dotted curve), and the entire sample (solid curve). For the latter, solid lines indicate the central value and values of the log likelihood corresponding to 1 statistical standard deviation.

reliability in a remarkably short time. The collaborating institutions thank SLAC for its support and the kind hospitality extended to them. This work has been supported by the U.S. Department of Energy and National Science Foundation, the Natural Sciences and Engineering Research Council (Canada), the Institute of High Energy Physics (China), Commissariat à l'Energie Atomique and Institut National de Physique Nucléaire et de Physique des Particules (France), Bundesministerium für Bildung und Forschung (Germany), Istituto Nazionale di Fisica Nucleare (Italy), the Research Council of Norway, the Ministry of Science and Technology of the Russian Federation, and the Particle Physics and Astronomy Research Council (United Kingdom). Individuals have received support from the Swiss National Foundation, the A. P. Sloan Foundation, the Research Corporation, and the Alexander von Humboldt Foundation.

*Also with Università di Perugia, Perugia, Italy.

†Also with Università della Basilicata, Potenza, Italy.

‡Deceased.

- [1] A. B. Carter and A. I. Sanda, Phys. Rev. D **23**, 1567 (1981); I. I. Bigi and A. I. Sanda, Nucl. Phys. **B193**, 85 (1981).
- [2] J. H. Christenson *et al.*, Phys. Rev. Lett. **13**, 138 (1964).
- [3] See, for example, L. Wolfenstein, Eur. Phys. J. C **15**, 115 (2000).
- [4] Particle Data Group, D. E. Groom *et al.*, Eur. Phys. J. C **15**, 1 (2000).
- [5] N. Cabibbo, Phys. Rev. Lett. **10**, 531 (1963); M. Kobayashi and T. Maskawa, Prog. Theor. Phys. **49**, 652 (1973).
- [6] Throughout this paper, flavor-eigenstate decay modes imply also their charge conjugate.
- [7] BABAR Collaboration, B. Aubert *et al.*, SLAC-PUB-8569 (to be published).
- [8] G. C. Fox and S. Wolfram, Phys. Rev. Lett. **41**, 1581 (1978).
- [9] OPAL Collaboration, K. Ackerstaff *et al.*, Eur. Phys. J. C **5**, 379 (1998); CDF Collaboration, T. Affolder *et al.*, Phys. Rev. D **61**, 072005 (2000); ALEPH Collaboration, R. Barate *et al.*, Phys. Lett. B **492**, 259 (2000).
- [10] See, for example, F. J. Gilman, K. Kleinknecht, and B. Renk, Eur. Phys. J. C **15**, 110 (2000).